

Full length article

Increasing the kinetic stability of bulk metallic glasses

J.Q. Wang^{a, b}, Y. Shen^b, J.H. Perepezko^{b, *}, M.D. Ediger^c^a Ningbo Institute of Materials Technology and Engineering, Chinese Academy of Science, Ningbo, Zhejiang 315201, China^b Department of Materials Science and Engineering, University of Wisconsin-Madison, Madison, WI 53706, USA^c Department of Chemistry, University of Wisconsin-Madison, Madison, WI 53706, USA

ARTICLE INFO

Article history:

Received 1 September 2015

Received in revised form

25 November 2015

Accepted 25 November 2015

Available online 12 December 2015

Keywords:

Metallic glasses

Glass transition

Relaxation

Kinetic stability

ABSTRACT

Metallic glasses are non-equilibrium materials and the glass transition temperature upon heating $T_{g,h}$ can be used to characterize the kinetic stability of the glass. Annealing below the glass transition is well-known to induce relaxation processes that reduce the glass enthalpy. We demonstrate that a liquid-cooled Au-based metallic glass can achieve very high kinetic stability by an optimal annealing treatment to yield a large increase in $T_{g,h}$ of 28 K; this is 3–5 times larger than the increase usually reported. The measured enthalpy decrease of 1100 J/mol is about 50% of the difference between the as-cooled glass and the equilibrium crystalline state and reaches the extrapolated enthalpy of the supercooled liquid. The optimal annealing conditions can be determined by an enthalpy-temperature-time (ETT) diagram which is proposed for the first time based on the comprehensive examination of relaxation processes. At equilibrium, a direct relation is established between the increase in kinetic stability as measured by the increase in $T_{g,h}$ and the enthalpy decrease.

© 2015 Acta Materialia Inc. Published by Elsevier Ltd. All rights reserved.

1. Introduction

Metallic glasses exhibit excellent physical and chemical properties, such as soft magnetic properties, good catalytic performance, high strength and good corrosion resistance [1–4]. However, as a result of their far-from-equilibrium nature, the properties of metallic glasses change with time as they relax towards low energy states. Increasing the kinetic stability of metallic glasses would extend their utility to higher temperatures. It has been found that the kinetic stability of glasses can be increased by using vapor deposition fabrication methods [5–11]. Vapor-deposited glasses can achieve low enthalpy and high kinetic stability as indicated by a long transformation time and an increase in $T_{g,h}$ (glass transition onset temperature measured on heating) [5–8,10–13]. Fast molecular/atomic mobility on the surface during deposition is believed to allow access to stable low energy states [5,6]. However, vapor deposition methods cannot be used to prepare bulk materials. An efficient approach towards bulk metallic glasses with high kinetic stability and low enthalpy has yet to be developed. An advance along these lines would not only supply important new materials, but also would provide a critical set of

comparisons with vapor-deposited ultrastable glasses and be helpful for exploring fundamental issues regarding amorphous materials.

It is well known that annealing glasses below the glass transition temperature can cause relaxation towards the equilibrium supercooled liquid. In this structural relaxation process, typically the kinetic stability increases while the enthalpy decreases. For example, Zhu et al. found that 7×10^5 s annealing at $0.89T_{g,h}$ can increase $T_{g,h}$ by about 8 K with an enthalpy decrease of about 23 J/g for $Zr_{52.5}Cu_{17.9}Ni_{14.6}Al_{10}Ti_5$ [14]. Kohda et al. found that 4.2×10^5 s annealing at $0.97T_{g,h}$ can increase $T_{g,h}$ by about 7 K with an enthalpy decrease of about 3 J/g for $Pt_{60}Ni_{15}P_{25}$ [15]. Haruyama et al. found that 6×10^5 s annealing at $0.94T_{g,h}$ can increase $T_{g,h}$ by about 13 K with an enthalpy decrease of about 5.5 J/g for $Pd_{42.5}Cu_{30}Ni_{7.5}P_{20}$ [16]. In other cases however, the enthalpy decrease that occurs during annealing is not accompanied by an increase in kinetic stability. For a $Pd_{42.5}Cu_{30}Ni_{7.5}P_{20}$ metallic glass, it was found that annealing for short times (<200 s) could lower both the enthalpy and the kinetic stability [16]. An $Au_{49}Cu_{26.9}Ag_{5.5}Pd_{2.3}Si_{16.3}$ metallic glass exhibited no obvious change in $T_{g,h}$ while the enthalpy decreased by about 3.7 J/g when annealed at $0.77T_{g,h}$ for one year [17]. A 20-million-year-old amber glass exhibited no obvious change in $T_{g,h}$ while the enthalpy decreased about 26 J/g [18]; in contrast, 110-million-year-old amber exhibits a 15 K increase in $T_{g,h}$ with an enthalpy decrease of only about 8 J/g [19]. The annealing

* Corresponding author.

E-mail address: perepezk@engr.wisc.edu (J.H. Perepezko).

effect on kinetic stability (i.e. increase of $T_{g,h}$) has not been studied sufficiently to understand this range of behavior. We expect that there are opportunities to increase the kinetic stability of metallic glasses by optimizing the annealing protocol.

Calorimetry has been a very effective method in measuring the phase transitions in glassy materials. A recently developed nano-calorimeter commercialized by Mettler-Toledo, Flash DSC 1, extends the heating rates up to 40,000 K/s and cooling rates up to 10,000 K/s [20–22]. The capability of heating so fast provides chances to observe some abnormal phase transition behaviors and studying the extreme kinetics of phase transition materials [8,23–26]. The capability of cooling so fast makes it possible to obtain glasses from liquids with poor glass-forming ability, such as metallic glasses, and study their thermal properties *in situ* [27,28]. Such an emerging powerful technique will provide chances to explore new materials and new properties of existing materials.

In this work, we studied the kinetic and thermodynamic characteristics of a liquid-cooled $\text{Au}_{49}\text{Cu}_{26.9}\text{Ag}_{5.5}\text{Pd}_{2.3}\text{Si}_{16.3}$ metallic glass (Au-MG) annealed for various times at temperatures in a range between $0.78T_{g,c}$ and $T_{g,c}$ ($T_{g,c}$ is the onset glass transition temperature upon cooling) using Flash DSC. The annealing time was varied across more than six orders of magnitude in these experiments. From a comprehensive examination of the temperature- and time-dependent behaviors, an enthalpy-temperature-time (ETT) diagram is obtained for the first time to show how the annealing temperature is combined optimally with the annealing time. Under optimal annealing a relation is established between the increase in kinetic stability and the decrease of glass enthalpy.

2. Experimental methods

Metallic glass ribbons with nominal composition of $\text{Au}_{49}\text{Cu}_{26.9}\text{Ag}_{5.5}\text{Pd}_{2.3}\text{Si}_{16.3}$ (at.%, a bulk glass former [29]) were prepared using an induction melter equipped with a spinning roller protected under an atmosphere of high-purity Ar gas. The tangent speed of the roller is 25 m/s. The thickness of the ribbon is about 30 μm and the width is about 2 mm. The thermal properties of the alloy were studied using a high-rate differential scanning calorimeter (Flash DSC 1, Mettler Toledo) [22]. During measurement, a flow of N_2 gas (15 ml/min) was applied to protect the sample from oxidation. The allowable sample mass for Flash DSC is between 10 ng and 1 μg . A representative Flash DSC trace in a cooling and heating cycle is shown in Fig. 1(a). The melting enthalpy of the tested sample is about $9.95 \pm 0.36 \mu\text{J}$. The specific melting enthalpy of the melt-spun Au-based MG is measured to be $40.2 \pm 0.4 \text{ J/g}$ using a Perkin Elmer Diamond DSC at a heating rate of 40 K/min. Thus, the mass of the Flash DSC sample is determined to be $9.95 \times 10^{-6} / 40.2 \text{ g} = (248 \pm 9) \times 10^{-9} \text{ g} [(1.95 \pm 0.07) \times 10^{-9} \text{ mole}]$.

To determine the critical cooling rate (R_c) for suppressing the crystallization upon cooling, various cooling rates were applied and the crystallization enthalpy (H_x) on subsequent heating was measured. For the sample cooled at high enough R , the H_x becomes a constant (about 7.4 μJ), which means the sample is completely amorphous. The R_c range is determined to be 900–1100 K/s, as shown in Fig. 1(b). In subsequent experiments, a cooling rate of 6000 K/s ($>R_c$) was employed to obtain completely amorphous samples. The $T_{g,c}$ was determined to be $439 \pm 1 \text{ K}$ for cooling rates between 2000 K/s and 10,000 K/s.

To study the stability of samples annealed at different temperatures and for various times, cycles of cooling-annealing-heating were applied for the same sample. A schematic figure illustrating one cycle of the above experimental procedure is shown in Fig. 2(a). A corresponding DSC heat flow trace is also shown in Fig. 2(b).

The alpha relaxation time (τ_α) at different temperatures was measured using two methods. At temperatures below 420 K, the

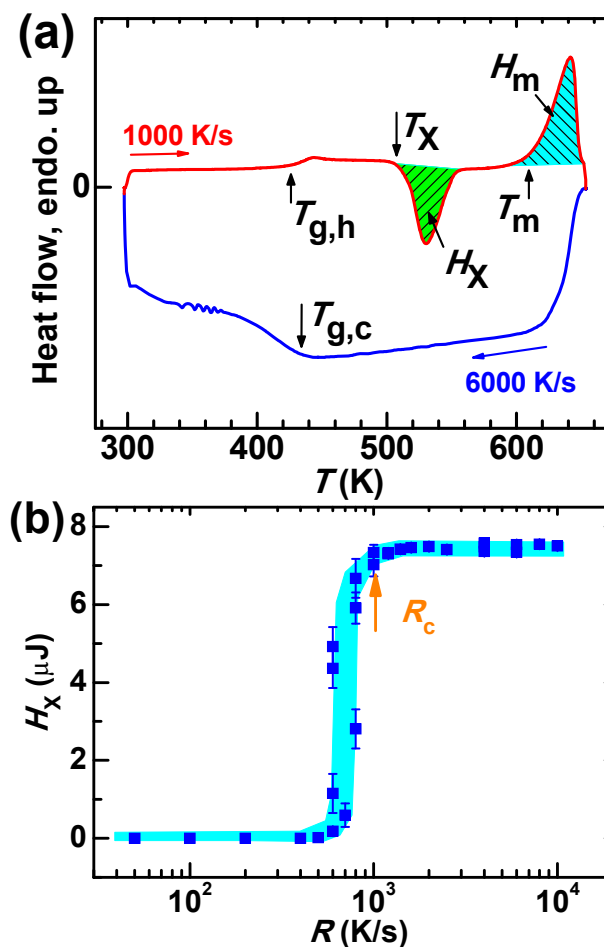


Fig. 1. (a) A representative Flash DSC trace upon heating (red) and cooling (blue). The heating rate is 1000 K/s and the cooling rate is 6000 K/s. Upon heating, the glass transition temperature ($T_{g,h}$), crystallization temperature (T_x), crystallization enthalpy (H_x), melting temperature (T_m), and melting enthalpy (H_m) can be determined. Upon cooling, the onset glass transition temperature ($T_{g,c}$) can be determined. (b) The H_x of the samples cooled at various cooling rates (R). The lowest cooling rate to obtain fully amorphous sample is defined as the critical cooling rate (R_c), which is about 1000 K/s. (For interpretation of the references to colour in this figure legend, the reader is referred to the web version of this article.)

time for the glass to relax to the supercooled liquid state is treated as equal to the τ_α [18]. At temperatures above 420 K, the τ_α was measured using an *ac* DSC measurement with a temperature oscillation amplitude of 1 K and a frequency range from 50 Hz to 1000 Hz. For a given frequency ($1/t_0$), the temperature was scanned from 408 K to 468 K. At low temperature, the sample responds as a glass with a low heat capacity, while at high temperatures, the sample responds as a liquid with a large heat capacity. The temperature where the sample transforms from a glass-like to liquid-like behavior at the given oscillation period t_0 is recognized as the temperature where $\tau_\alpha = t_0/2\pi$.

To determine the glass-to-liquid transition time (t_{trans}) for a glass in a low energy state, the temperature is first raised to the destination temperature (at 6000 K/s) and then held isothermally. During isothermal annealing, *ac* DSC measurement (amplitude: 1 K) was applied to determine the time when the glass transforms completely to a liquid. The isothermal *ac* method was used to measure the t_{trans} at temperatures of 428 K, 433 K, 438 K and 448 K. The data at about 460 K were measured by heating the metallic glass continuously at 1000 K/s. The peak temperature of the C_p

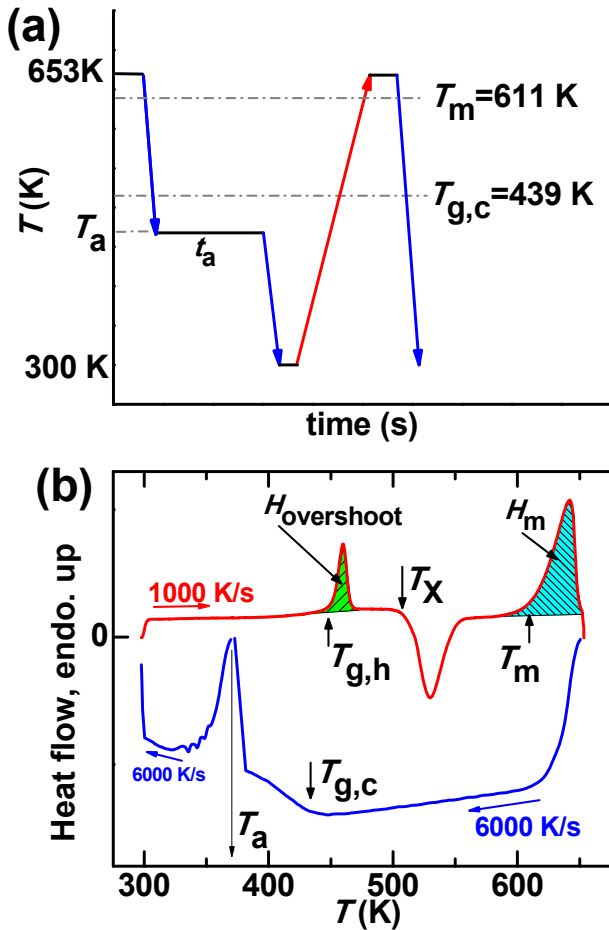


Fig. 2. (a) Schematic illustration for the isothermal annealing experiments. The melt was first cooled fast (6000 K/s) to the destination temperature (T_a , e.g. 373 K), held isothermally for some time ($t_a = 0.05\text{--}10^5$ s), cooled to room temperature (298 K), held isothermally for 2 s, and then heated again at 1000 K/s up to melting temperature to measure the glass transition and crystallization of the annealed sample. (b) Representative Flash DSC traces measured in above procedure. This sample was annealed at 373 K for 30,000 s.

overshoot is about 460 K and is treated as the transition temperature. The time from the onset to the endset of the overshoot is treated approximately as the t_{trans} .

3. Results

Representative DSC curves of the heat capacity (C_p) for samples annealed at 373 K for various times are shown in Fig. 3(a). As the annealing time increases, the C_p overshoot at the glass transition increases and the glass transition onset temperature ($T_{g,h}$) also increases accordingly with a maximum increase of 28 K. The C_p and crystallization temperature (T_x) of the supercooled liquid do not change which denotes that the supercooled liquids are in the same equilibrium state and the annealed glasses are fully amorphous. The enthalpy of the sample [including that of the glass (H_G), the liquid (H_L) and the crystal (H_C)] is obtained by integrating the heat capacity, as shown in Fig. 3(b). The H_L is fitted using a polynomial equation, $H_L = -25.8 + 0.093T - 6.2 \times 10^{-5}T^2 + 3 \times 10^{-8}T^3$ [with H_L in kJ/mol and T in K, see the orange solid curve (in the web version) in Fig. 3(b)]. The H_C is fitted by a linear equation, $H_C = -13.2 + 0.038T$ [with H_C in kJ/mol and T in K, the black dash-dotted line in Fig. 3(b)]. To more clearly show the change of H_G with

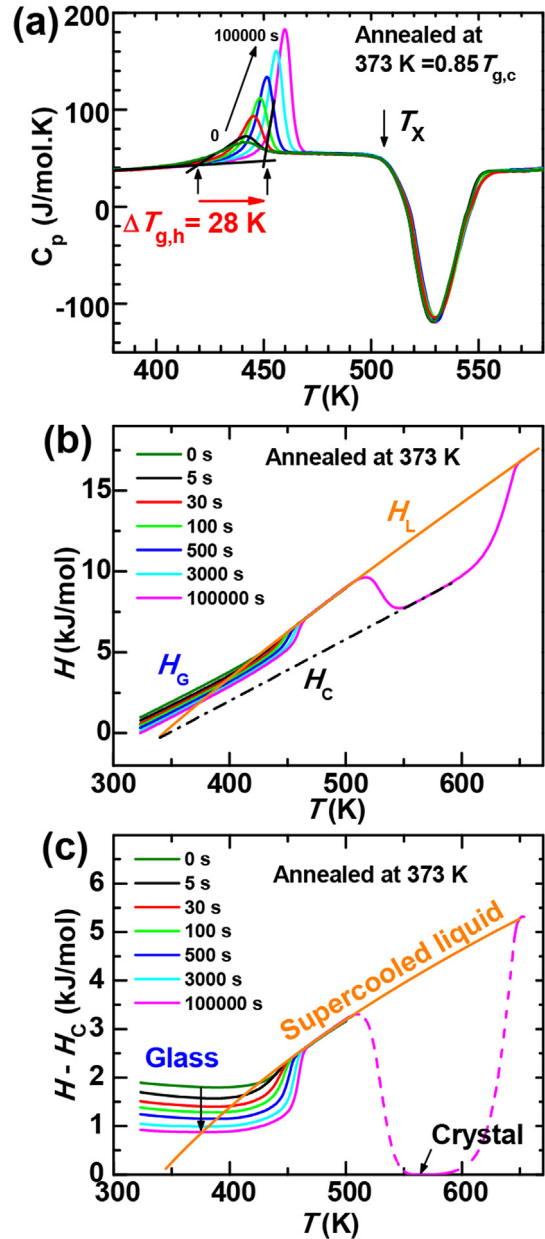


Fig. 3. (a) Heat capacity, C_p , for the samples annealed at 373 K ($= 0.85T_{g,c}$) for various times (0– 10^5 s). The onset glass transition temperature ($T_{g,h}$) and crystallization (T_x) are marked by arrows. The $T_{g,h}$ increases by 28 K from 424 K to 452 K after being annealed for 10^5 s. (b) The enthalpy of annealed samples. (c) The relative enthalpy of annealed samples obtained by subtracting H_C .

annealing, H_G is presented relative to H_C in Fig. 3(c). The enthalpy of the glass decreases gradually upon annealing until it reaches halfway to the enthalpy of the equilibrium crystalline state.

The enthalpy change (ΔH) of the metallic glass during annealing is shown versus the annealing temperature and time in Fig. 4. First, to measure the ΔH dependence on temperature (T), the sample was annealed at various temperatures for a constant time, as shown in Fig. 4(a). For a given annealing time, ΔH reaches a minimum at a temperature (T_{min}) below $T_{g,c}$. The T_{min} decreases as the annealing time increases. Although the ΔH on the low temperature side decreases systematically, it does not keep decreasing on the high temperature side, but merges into a single curve when the annealing time is long enough. In addition, to measure the

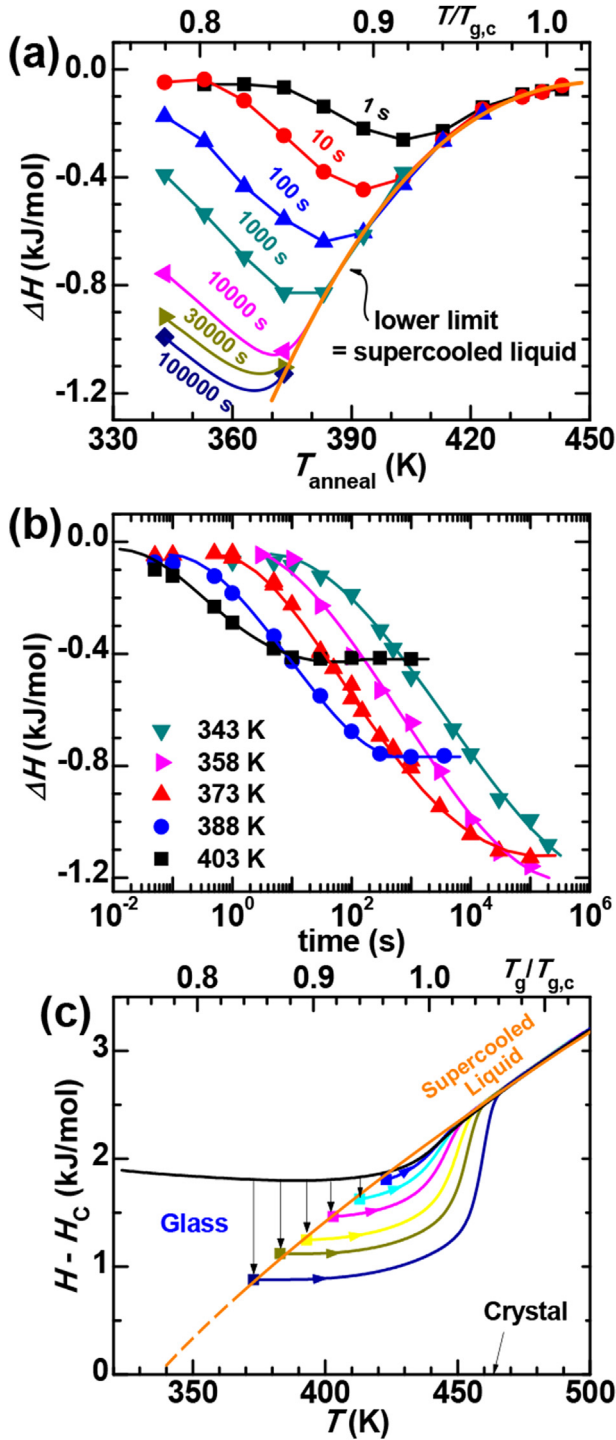


Fig. 4. (a) The enthalpy decrease (ΔH) for glasses annealed at different temperatures for fixed times. (b) The ΔH for the glasses annealed at 5 representative temperatures (343, 358, 373, 388, and 403 K) for various times. The solid curves in (a) and (b) are plotted as guides. (c) The enthalpy of fully-relaxed glasses (solid symbols) falls onto the extrapolation of the supercooled liquid enthalpy (orange curve). The temperature-dependent enthalpies of the fully-relaxed glasses measured on heating are shown as solid curves. The enthalpy of the as-cooled glass measured on heating (black curve) is shown for comparison. (For interpretation of the references to colour in this figure legend, the reader is referred to the web version of this article.)

dependence of ΔH on annealing time, the sample was annealed for various times at a given temperature, as shown in Fig. 4(b). For example, at 403 K, ΔH initially decreases with increasing annealing

time and then becomes constant.

It is noteworthy that ΔH merges on the high temperature side in Fig. 4(a) and becomes constant when the annealing time is long enough in Fig. 4(b). The enthalpies of these fully-relaxed glasses are shown as the filled symbols in Fig. 4(c). All these data are consistent with the extrapolation of the enthalpy of the supercooled liquid from higher temperatures. This indicates that the lower limit on the right-hand side (orange curve) in Fig. 4(a) and the long-time plateaus in Fig. 4(b) represent the equilibrium supercooled liquid. As shown in Fig. 4(a), the maximum loss in enthalpy in a given time occurs at temperatures where the sample does not reach equilibrium. The optimal combination of annealing temperature and annealing time for obtaining the lowest enthalpy glass is determined by both the relaxation kinetics and the position of the metastable equilibrium state. Analogous results have been obtained for vapor-deposited glasses; in this case, substrate temperature corresponds to annealing temperature and deposition rate corresponds to the inverse of the annealing time [10–12].

To provide a conceptual picture of the evolution of enthalpy during annealing, 2-dimensional and 3-dimensional plots of ΔH versus annealing temperature and annealing time are shown in Fig. 5. Upon annealing, the enthalpy of the glass decreases due to physical aging. When the annealing time is long enough, the enthalpy becomes constant which represents the equilibrium supercooled liquid (ESL) state. The time for the glass to relax to the ESL increases with decreasing temperature. The ESL state is metastable and the samples will eventually crystallize. We note that many previous investigations have annealed glasses isothermally to obtain the crystallization temperature-time-transformation (TTT) diagram to evaluate glass forming ability. However, less information has been obtained about what happens during the isothermal annealing process before crystallization. Fig. 5(b) shows that the sample experiences two stages before crystallization: the first is a nonequilibrium relaxation stage (glass) and the second is a metastable equilibrium stage (extrapolation of supercooled liquid).

The determination of alpha relaxation time ($\tau_\alpha = 0.0032$ s) using AC measurement is shown in Fig. 6(a) and (b). The determination of the isothermal glass-to-liquid transition time (t_{trans}) at 428 K for the highly stable glass that equilibrated at 373 K is shown in Fig. 6(c) and (d). The τ_α and the t_{trans} for the glasses equilibrated at 373 K and 388 K are shown in Fig. 6(e). For a given temperature, the t_{trans} is much larger than τ_α , which denotes a high kinetic stability. According to Tool-Narayanaswamy-Moynihan (TNM) model [30], the isothermal time evolution of fictive temperature (T_f , the cross temperature of the glass enthalpy and liquid enthalpy) or glass enthalpy (H) following a single temperature step from equilibrium (T_0) at time t_1 can be described using a relaxation function

$$T_f(t) = T_0 + \Delta T [1 - \phi(t - t_1, t)] \quad (1)$$

where t is relaxation time at temperature $T_0 + \Delta T$, T_0 is the temperature of the initial equilibrium state, $\phi(t - t_1, t)$ is both a non-exponential and a nonlinear function which can be expressed as

$$\phi(t - t_1, t) = \exp \left[- \left(\int_{t_1}^t dt / \tau_0 \right)^\beta \right] \quad (2)$$

where $0 < \beta \leq 1$; a smaller β denotes a broader distribution of the spectrum of relaxation times. The relaxation time τ_0 is given as

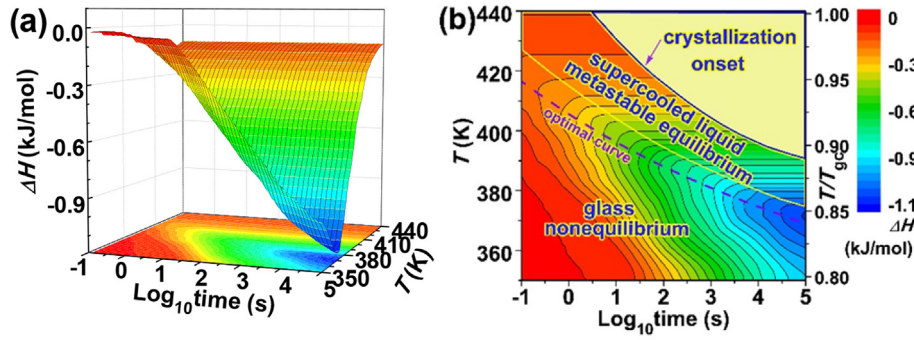


Fig. 5. (a) The 3-dimensional plot of enthalpy decrease (ΔH) versus isothermal annealing time (logarithmic) and annealing temperatures. (b) The 2-dimensional contours of the ΔH . Each contour (from red to blue) represents a 50 J/mol decrease. From lower-left to upper-right, the diagram can be divided into two zones before crystallization: the nonequilibrium glass state and the metastable equilibrium supercooled liquid state. The dashed curve shows the optimal annealing temperatures to achieve the lowest enthalpy for a given annealing time. (For interpretation of the references to colour in this figure legend, the reader is referred to the web version of this article.)

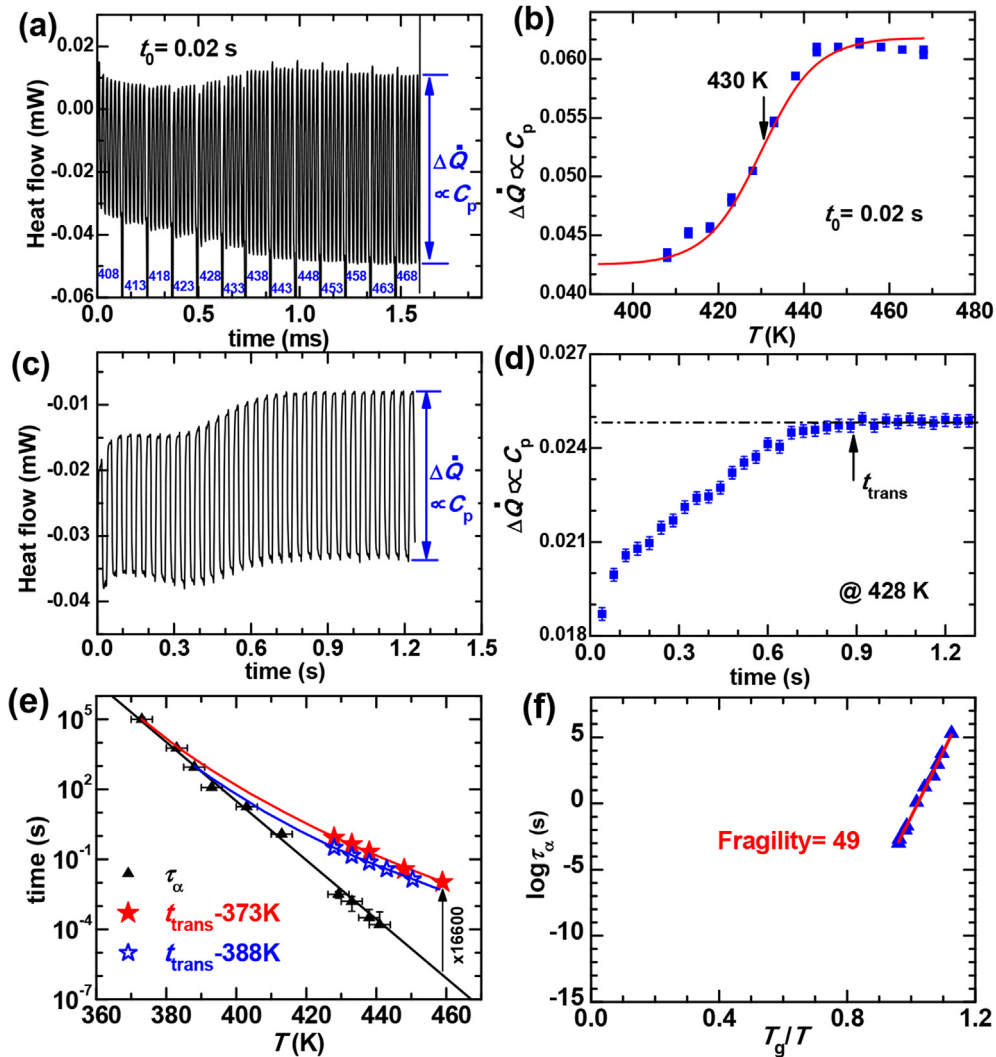


Fig. 6. (a) The ac measurement of the α -relaxation time ($\tau_\alpha = t_0/2\pi = 0.0032$ s). At each temperature (from 408 K to 468 K), 5 oscillation periods were measured. The heat flow amplitude (ΔQ) is proportional to the heat capacity (C_p). (b) The ΔQ is shown versus the temperature. The temperature where $\tau_\alpha = t_0/2\pi = 0.0032$ s is determined to be about 430 K. (c) The measurement of glass-to-liquid de-aging transition time (t_{trans}) at 428 K using ac method; this sample had been annealed for 10^5 s at 373 K. (d) The t_{trans} is determined to be about 0.88 s according to the evolution of ΔQ which is proportional to the heat capacity. (e) The τ_α (black filled triangles) and t_{trans} versus temperature for the highly stable glasses equilibrated at 373 K (red filled stars) and 388 K (blue open stars). The curves are the TNM fitting results. (f) The Angell plot of τ_α versus T_g/T determines the fragility of the $Au_{49}Cu_{26.9}Ag_{5.5}Pd_{2.3}Si_{16.3}$ glass forming liquid to be about 49. (For interpretation of the references to colour in this figure legend, the reader is referred to the web version of this article.)

$$\tau_0 = A \exp \left[x \frac{\Delta h}{RT} + (1-x) \frac{\Delta h}{RT_f} \right] \quad (3)$$

where A , x ($0 \leq x \leq 1$), and Δh are constants, and R is the gas constant. A is the extrapolated time according to the Arrhenius equation representing the characteristic time at infinite high temperature. The x partitions the material dependence between temperature and structure (T_f). The Δh is the activation enthalpy for the relaxation process and expresses the temperature dependence of the relaxation time for the linear regime close to equilibrium:

$$\Delta h = R \lim_{T_f \rightarrow T} \left(\frac{\partial \ln \tau_0}{\partial (1/T)} \right) \equiv R \frac{\partial \ln \tau_{0e}}{\partial (1/T)} \quad (4)$$

where τ_{0e} is the characteristic relaxation time in the equilibrium state and is equal to the τ_α shown in Fig. 6(f). The value of A and Δh can be determined from Fig. 6(f) as $A = 10^{-51 \pm 1}$ s and $\Delta h = 395 \pm 8$ kJ/mol. The kinetic fragility m of the glass-forming liquid is determined to be about 49 ± 1 according to the Angell plot of τ_α , as is shown in Fig. 6(f) [31].

4. Discussion

During isothermal annealing, the nonequilibrium glass always relaxes towards the equilibrium supercooled liquid state. The relaxation can be divided into two types: the aging when $H_C > H_L$ and the de-aging when $H_C < H_L$ [18,32]. The isothermal transition time (t_{trans}) from glass to liquid is related to the alpha-relaxation time (τ_α , the rearrangement time of atoms or molecules in the equilibrium state). That is, $t_{\text{trans}} \leq \tau_\alpha$ for aging, and $t_{\text{trans}} > \tau_\alpha$ for de-aging [18]. Upon heating, the ordinary glass that was quenched directly from a liquid will transform quickly into liquid when its enthalpy meets that of the supercooled liquid, which denotes that the t_{trans} is comparable to τ_α . A typical character of ultrastable glasses is that the t_{trans} is much longer than the τ_α in the de-aging state [33], see Fig. 6(e). The glass equilibrated at 388 K has a smaller t_{trans} compared to the glass equilibrated at 373 K, which denotes a smaller kinetic stability and is consistent with the higher enthalpy of this glass. The t_{trans} of the Au-MG equilibrated at 373 K is about 10^2 – $10^{4.2}$ higher than τ_α , which is similar to that reported for vapor-deposited ultrastable glasses, although for the most stable vapor-deposited glasses these results were obtained for larger values of τ_α [33]. The t_{trans} values can be well fitted using the TNM model [30], as shown by the solid curves in Fig. 6(e). The fitting parameters are determined to be $\beta = 0.45$, $x = 0.5$ for the glass equilibrated at 373 K, and $\beta = 0.7$, $x = 0.6$ for the glass equilibrated at 388 K. The glass in equilibrium at 373 K exhibits a stronger dependence on the fictive temperature T_f and is less dependent on temperature (the parameter x in Eq. (3) is smaller) compared to the glass in equilibrium at 383 K, which also denotes higher stability.

The increase of kinetic stability (e.g. higher $T_{g,h}$) combined with the decrease in enthalpy has been widely observed in vapor-deposited ultrastable glasses [5–7,10–13]. However, the quantitative relationship between kinetic stability and enthalpy has not been systematically investigated for bulk metallic glasses. It is valuable to examine the relation between $T_{g,h}$ and enthalpy for the present annealed metallic glass. The $T_{g,h}$ is plotted versus the glass enthalpy change (ΔH) for the samples annealed at various T and for various times, as shown in Fig. 7. When the annealing temperature is well below $T_{g,c}$, e.g. 358 K, the $T_{g,h}$ will first decrease along with the decrease of enthalpy upon annealing which can be found in Fig. 7(a) and other works [17,34]. For further annealing, the $T_{g,h}$ increases along with the decrease of enthalpy, which can be found

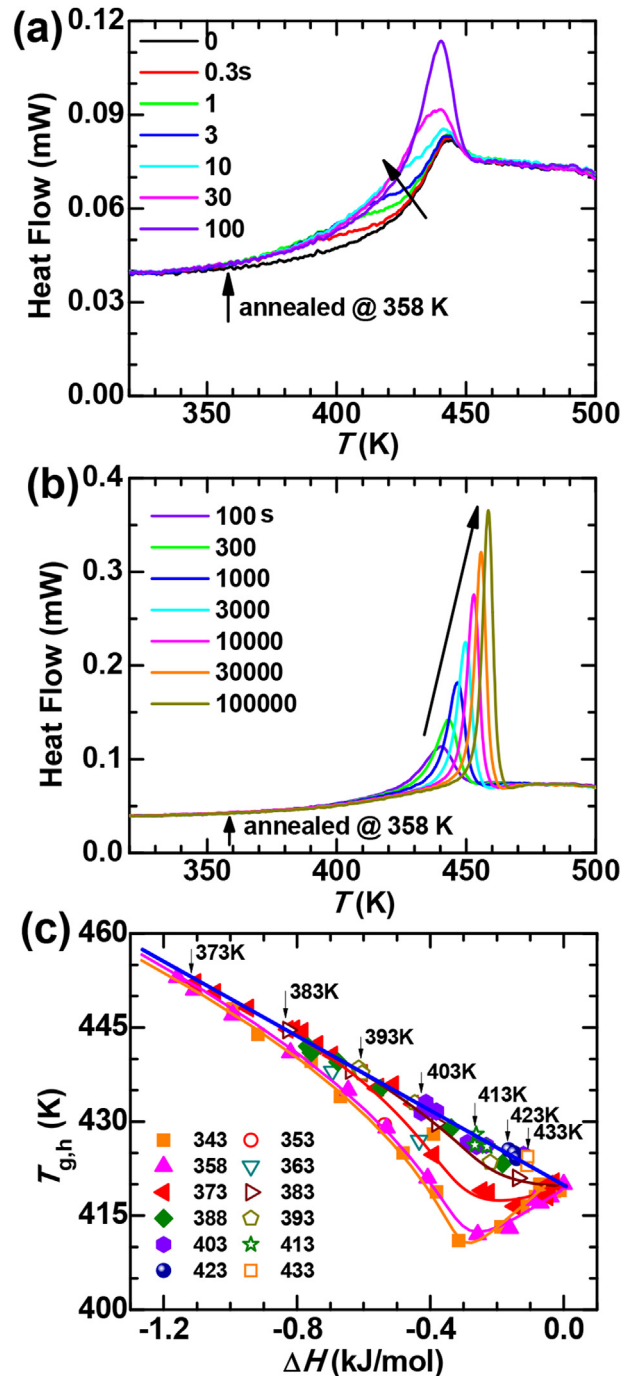


Fig. 7. (a) The DSC traces for the samples annealed at 358 K for short times (≤ 100 s), in which both $T_{g,h}$ and enthalpy decrease upon annealing. (b) The DSC traces for the samples annealing at 358 K for long times (≥ 100 s), in which the $T_{g,h}$ increases while the enthalpy decreases upon annealing. (c) The $T_{g,h}$ versus the enthalpy change (ΔH) for samples annealed at various temperatures. The arrows mark the maximum change of $T_{g,h}$ and ΔH at each annealing temperature. When annealing at low temperatures, i.e. 358 K, the $T_{g,h}$ will first decrease and then increase when enthalpy decreases upon annealing. The curves are plotted to guide eyes.

in Fig. 7(b). When the annealing time is long enough, the dependence of $T_{g,h}$ on ΔH tends to merge with the data that annealed slightly below $T_{g,c}$. When the annealing temperature is slightly below $T_{g,c}$, the $T_{g,h}$ will increase along with the decrease of enthalpy upon annealing. There exists a maximum value for the increase of $T_{g,h}$ and the decrease of enthalpy, as is marked by the arrows in

Fig. 7(c); this occurs when the sample reaches the equilibrium supercooled liquid state. These values of $T_{g,h}$ have a linear relation with ΔH with a slope of about $dT_{g,h}/dH = -29.7(\pm 0.5)$ mol.K/kJ.

It is interesting to note that the kinetic stability decreases ($T_{g,h}$ decreases) while the thermodynamic stability increases (enthalpy decreases) for short-time annealing at low temperatures. Such behavior has also been observed in another Pd-based metallic glass and has been associated with volume dilatation during short-time annealing at low temperatures [16]. This can be elucidated in terms of the two-components model that includes positive as well as negative fluctuations in local density [16]. Such a decrease in enthalpy has been attributed to the slow- β relaxation [17,34], which derives from local rearrangements of atoms. However, when the glass gets to equilibrium after a long-time annealing at low temperatures or being annealed close to glass transition temperature, the α -relaxation (universal rearrangement of nearest-neighbor structure) takes over. Thus, we propose that the α -relaxation process causes an increase in kinetic stability and decrease in enthalpy, while the slow- β relaxation can only induce a decrease in enthalpy.

Annealing glasses below the glass transition temperature has been widely studied and has been applied to release the residual stress [14,16,35–38]. A large increase in $T_{g,h}$ by about 13 K was observed in polymer glasses [35,36]. However, the change of $T_{g,h}$ for metallic glasses is usually less than 10 K [14,15,32,37,38], which was attributed to the low fragility of the glass forming liquid [9]. The large increase in $T_{g,h}$ by 28 K obtained here is about 3–5 times larger than previously reported values for metallic glass relaxation. As is shown in Fig. 4(a), if the annealing temperature (T_a) is too high, the small enthalpy difference between the as-cooled glass and the equilibrium supercooled liquid limits the increase of kinetic stability. As is shown in Fig. 7, if the annealing temperature is too low, short-time annealing ($t_a \ll \tau_\alpha$) can decrease the glass enthalpy but will not increase $T_{g,h}$, which can be attributed to the heterogeneous nature of slow- β relaxation [18,17,39]. To obtain the largest increase in stability at a given annealing time (t_a), the optimal annealing temperature for this Au-MG is 6–10 K lower than the temperature where $\tau_\alpha = t_a$. The optimal annealing curve can be expressed by the Vogel–Fulcher–Tammann equation as $T_a = 274 + 132/\log(t_a)$, as is shown by the dashed curve in Fig. 5(b). Using the optimal annealing method, we also obtained high kinetic stability starting from the as-spun ribbon, as shown in Fig. 8. Thus, the high stability can be attributed to the optimal combination of annealing temperature and annealing time, regardless of the sample fabrication method.

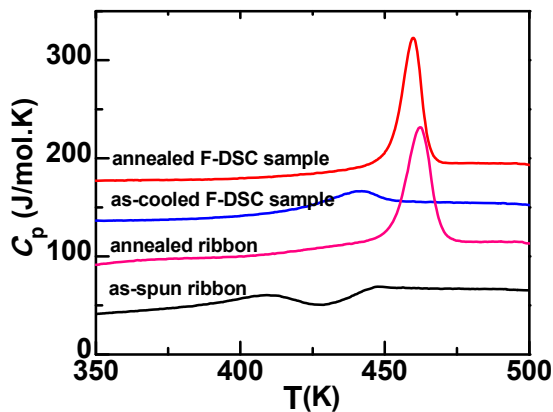


Fig. 8. DSC traces of the glass transition behavior of the as-spun ribbon, the ribbon annealed at 373 K for 10^5 s (annealed ribbon), the sample cooled in-situ at 6000 K/s using Flash DSC (as-cooled F-DSC sample), and the sample annealed in-situ at 373 K for 10^5 s (annealed F-DSC sample). The curves have been shifted vertically for comparison.

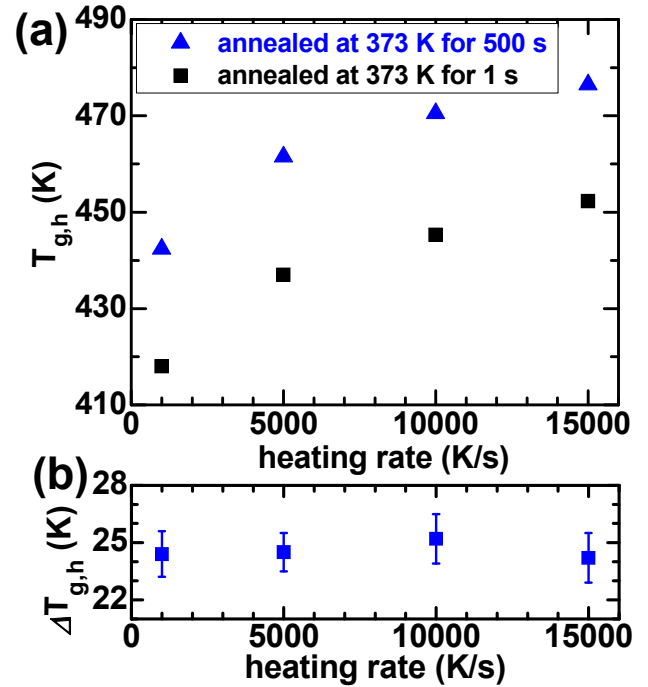


Fig. 9. (a) The heating rate dependent behavior of $T_{g,h}$ for glasses at two different states: one is more stable (annealed at 373 K for 500 s) than the other (annealed at 373 K for 1 s). The enthalpy difference between the two samples is about 0.7 kJ/mol. The sample annealed for 500 s exhibit 24.5 K higher $T_{g,h}$ compared to the sample annealed for only 1 s. (b) The change of $T_{g,h}$ doesn't show obvious dependence on heating rate.

When fabricating ultrastable glasses using vapor deposition, elevated atomic mobility within the surface layer (several nanometers) plays a key role in promoting the rearrangement of atoms to approach their equilibrium configurations [6,40–42]. Vapor deposition is very inefficient for fabricating thick samples or bulk glasses. In contrast, the melt-spun Au-MG samples studied here have a thickness of about 25 μm . The optimal annealing method identified in this paper is not limited to ribbons but is also applicable for liquid-cooled bulk metallic glasses. The heating rate dependence of the $T_{g,h}$ for a highly stable glass is also studied, as is shown in Fig. 9. Compared to a less stable glass, the $T_{g,h}$ for the highly stable glass exhibits the same heating rate dependent behavior. This denotes that the large increase of $T_{g,h}$ by 28 K observed in this work does not derive from the heating rate effect.

5. Conclusion

We have demonstrated that liquid-cooled metallic glasses can be fabricated with very high kinetic stability (e.g., high $T_{g,h}$). In order to achieve high kinetic stability from liquid-cooled glasses, the optimal combination of annealing temperature and annealing time is of vital importance. The relationship between the glass-to-liquid transition temperature/time and enthalpy states has been studied systematically. We propose that the α -relaxation process causes an increase in kinetic stability and decrease in enthalpy, while the slow- β relaxation can only induce a decrease in enthalpy. A linear relationship is established between the increase in kinetic stability as measured by the increase in $T_{g,h}$ and the enthalpy decrease for the equilibrated glasses. While these results are specific to this Au-based MG, we expect that similar increases in kinetic stability can be obtained for many other metallic glasses and that this can widen the temperature range for applications.

Acknowledgments

Financial support from the NSF (DMR-1121288, CHE-1265737, DMR-1005334 and DMR-1332851) is gratefully acknowledged. JQW also acknowledges the support from One Hundred Talents Program of Chinese Academy of Science.

References

- [1] A. Inoue, A. Takeuchi, Recent development and application products of bulk glassy alloys, *Acta Mater.* 59 (2011) 2243–2267.
- [2] W.H. Wang, Bulk metallic glasses with functional physical properties, *Adv. Mater.* 21 (2009) 4524–4544.
- [3] J.Q. Wang, Y.H. Liu, M.W. Chen, D.V. Louzguine-Luzgin, A. Inoue, J.H. Perepezko, Excellent capability in degrading azo dyes by MgZn-based metallic glass powders, *Sci. Rep.* 2 (2012).
- [4] M. Carmo, R.C. Sekol, S.Y. Ding, G. Kumar, J. Schroers, A.D. Taylor, Bulk metallic glass nanowire architecture for electrochemical applications, *ACS Nano* 5 (2011) 2979–2983.
- [5] S.F. Swallen, K.L. Kearns, M.K. Mapes, Y.S. Kim, R.J. McMahon, M.D. Ediger, T. Wu, L. Yu, S. Satija, Organic glasses with exceptional thermodynamic and kinetic stability, *Science* 315 (2007) 353–356.
- [6] A. Sepulveda, E. Leon-Gutierrez, M. Gonzalez-Silveira, C. Rodriguez-Tinoco, M.T. Clavaguera-Mora, J. Rodriguez-Viejo, Accelerated aging in ultrathin films of a molecular glass former, *Phys. Rev. Lett.* 107 (2011).
- [7] A. H, D.P.B. Aji, F. Zhu, P. Liu, K.M. Reddy, S. Song, Y.H. Liu, T. Fujita, S. Kohara, M.W. Chen, Ultrastrong and ultrastable metallic glass, *ArXiv:1306.1575* (2013).
- [8] J.Q. Wang, N. Chen, P. Liu, Z. Wang, D.V. Louzguine-Luzgin, M.W. Chen, J.H. Perepezko, The ultrastable kinetic behavior of an Au-based nanoglass, *Acta Mater.* 79 (2014) 30–36.
- [9] H.B. Yu, Y.S. Luo, K. Samwer, Ultrastable metallic glass, *Adv. Mater.* 25 (2013) 5904–5908.
- [10] K.L. Kearns, S.F. Swallen, M.D. Ediger, T. Wu, Y. Sun, L. Yu, Hiking down the energy landscape: progress toward the Kauzmann temperature via vapor deposition, *J. Phys. Chem. B* 112 (2008) 4934–4942.
- [11] S.L.L.M. Ramos, M. Oguni, K. Ishii, H. Nakayama, Character of devitrification, viewed from enthalpic paths, of the vapor-deposited ethylbenzene glasses, *J. Phys. Chem. B* 115 (2011) 14327–14332.
- [12] K. Dawson, L. Zhu, L.A. Kopff, R.J. McMahon, L. Yu, M.D. Ediger, Highly stable vapor-deposited glasses of four tris-naphthylbenzene isomers, *J. Phys. Chem. Lett.* 2 (2011) 2683–2687.
- [13] I. Lyubimov, M.D. Ediger, J.J. de Pablo, Model vapor-deposited glasses: growth front and composition effects, *J. Chem. Phys.* 139 (2013).
- [14] Z.G. Zhu, P. Wen, D.P. Wang, R.J. Xue, D.Q. Zhao, W.H. Wang, Characterization of flow units in metallic glass through structural relaxations, *J. Appl. Phys.* 114 (2013).
- [15] M. Kohda, O. Haruyama, T. Ohkubo, T. Egami, Kinetics of volume and enthalpy relaxation in Pt60Ni15P25 bulk metallic glass, *Phys. Rev. B* 81 (2010).
- [16] O. Haruyama, T. Mofate, K. Morita, N. Yamamoto, H. Kato, T. Egami, Volume and enthalpy relaxation in Pd42.5Cu30Ni7.5P20 bulk metallic glass, *Mater. Trans.* 55 (2014) 466–472.
- [17] Z. Evenson, S.E. Naleway, S. Wei, O. Gross, J.J. Kruzic, I. Gallino, W. Possart, M. Stommel, R. Busch, Beta relaxation and low-temperature aging in a Au-based bulk metallic glass: from elastic properties to atomic-scale structure, *Phys. Rev. B* 89 (2014).
- [18] J. Zhao, S.L. Simon, G.B. McKenna, Using 20-million-year-old amber to test the super-Arrhenius behaviour of glass-forming systems, *Nat. Commun.* 4 (2013).
- [19] T. Perez-Castaneda, R.J. Jimenez-Rioboo, M.A. Ramos, Two-level systems and boson peak remain stable in 110-million-year-old amber glass, *Phys. Rev. Lett.* 112 (2014).
- [20] E. Zhuravlev, C. Schick, Fast scanning power compensated differential scanning nano-calorimeter: 1. The device, *Thermochim. Acta* 505 (2010) 1–13.
- [21] E. Zhuravlev, C. Schick, Fast scanning power compensated differential scanning nano-calorimeter: 2. Heat capacity analysis, *Thermochim. Acta* 505 (2010) 14–21.
- [22] V. Mathot, M. Pyda, T. Pijpers, G. Vanden Poel, E. van de Kerkhof, S. van Herwaardeng, F. van Herwaardeng, A. Leenaers, The Flash DSC 1, a power compensation twin-type, chip-based fast scanning calorimeter (FSC): first findings on polymers, *Thermochim. Acta* 522 (2011) 36–45.
- [23] K.L. Kearns, K.R. Whitaker, M.D. Ediger, H. Huth, C. Schick, Observation of low heat capacities for vapor-deposited glasses of indomethacin as determined by AC nanocalorimetry, *J. Chem. Phys.* 133 (2010).
- [24] J. Orava, A.L. Greer, B. Gholipour, D.W. Hewak, C.E. Smith, Characterization of supercooled liquid Ge2Sb2Te5 and its crystallization by ultrafast-heating calorimetry, *Nat. Mater.* 11 (2012) 279–283.
- [25] B. Yang, J.H. Perepezko, J.W.P. Schmelzer, Y.L. Gao, C. Schick, Dependence of crystal nucleation on prior liquid overheating by differential fast scanning calorimeter, *J. Chem. Phys.* 140 (2014).
- [26] J.H. Perepezko, C. Santhaweesuk, J.Q. Wang, S.D. Imhoff, Kinetic competition during glass formation, *J. Alloys Compd.* 615 (2014) S192–S197.
- [27] S. Pogatscher, D. Leutenegger, A. Hagmann, P.J. Uggowitzer, J.F. Löffler, Characterization of bulk metallic glasses via fast differential scanning calorimetry, *Thermochim. Acta* 590 (2014) 84–90.
- [28] J.H. Perepezko, T.W. Glendenning, J.Q. Wang, Nanocalorimetry measurements of metastable states, *Thermochim. Acta* 603 (2015) 24–28.
- [29] J. Schroers, B. Lohwongwatana, W.L. Johnson, A. Peker, Gold based bulk metallic glass, *Appl. Phys. Lett.* 87 (2005).
- [30] C.T. Moynihan, P.B. Macedo, C.J. Montrose, P.K. Gupta, M.A. DeBolt, J.F. Dill, B.E. Dom, P.W. Drake, A.J. Easteal, P.B. Elterman, R.P. Moeller, H. Sasabe, J.A. Wilder, Structural relaxation in vitreous materials, *Ann. N. Y. Acad. Sci.* 279 (1976) 15–35.
- [31] C.A. Angell, Formation of glasses from liquids and biopolymers, *Science* 267 (1995) 1924–1935.
- [32] S.S. Tsao, F. Spaepen, Structural relaxation of a metallic-glass near equilibrium, *Acta Metall.* 33 (1985) 881–889.
- [33] K. Dawson, L.A. Kopff, L. Zhu, R.J. McMahon, L. Yu, R. Richert, M.D. Ediger, Molecular packing in highly stable glasses of vapor-deposited tris-naphthylbenzene isomers, *J. Chem. Phys.* 136 (2012).
- [34] Z. Evenson, T. Koschine, S. Wei, O. Gross, J. Bednarcik, I. Gallino, J.J. Kruzic, K. Ratzke, F. Faupel, R. Busch, The effect of low-temperature structural relaxation on free volume and chemical short-range ordering in a Au49Cu26.9Si16.3Ag5.5Pd2.3 bulk metallic glass, *Scr. Mater.* 103 (2015) 14–17.
- [35] V.M. Boucher, D. Cangialosi, A. Alegria, J. Colmenero, Enthalpy recovery of glassy polymers: dramatic deviations from the extrapolated liquid like behavior, *Macromolecules* 44 (2011) 8333–8342.
- [36] D. Cangialosi, V.M. Boucher, A. Alegria, J. Colmenero, Direct evidence of two equilibration mechanisms in glassy polymers, *Phys. Rev. Lett.* 111 (2013).
- [37] Z. Evenson, R. Busch, Equilibrium viscosity, enthalpy recovery and free volume relaxation in a Zr44Ti11Ni10Cu10Be25 bulk metallic glass, *Acta Mater.* 59 (2011) 4404–4415.
- [38] G. Kumar, D. Rector, R.D. Conner, J. Schroers, Embrittlement of Zr-based bulk metallic glasses, *Acta Mater.* 57 (2009) 3572–3583.
- [39] Y.Z. Yue, C.A. Angell, Clarifying the glass-transition behaviour of water by comparison with hyperquenched inorganic glasses, *Nature* 427 (2004) 717–720.
- [40] C.W. Brian, L. Zhu, L. Yu, Effect of bulk aging on surface diffusion of glasses, *J. Chem. Phys.* 140 (2014).
- [41] Z.H. Yang, Y. Fujii, F.K. Lee, C.H. Lam, O.K.C. Tsui, Glass transition dynamics and surface layer mobility in unentangled polystyrene films, *Science* 328 (2010) 1676–1679.
- [42] E. Leon-Gutierrez, G. Garcia, A.F. Lopeandia, M.T. Clavaguera-Mora, J. Rodriguez-Viejo, Size effects and extraordinary stability of ultrathin vapor deposited glassy films of toluene, *J. Phys. Chem. Lett.* 1 (2010) 341–345.